Brief Communications

A Membrane Pool Retrieved via Endocytosis Overshoot at Nerve Terminals: A Study of Its Retrieval Mechanism and Role

Lei Xue, Benjamin D. McNeil, Xin-Sheng Wu, Fujun Luo, Liming He, and Ling-Gang Wu

National Institute of Neurological Disorders and Stroke, Bethesda, Maryland 20892

Endocytosis overshoot, which retrieves more membrane than vesicles just being exocytosed, occurs at nerve terminals and non-neuronal secretory cells. The mechanism that retrieves the overshoot membrane pool and the role of this pool remain largely unknown. We addressed this issue at the rat calyx of Held nerve terminal with capacitance measurements. We found that every calyx contained an overshoot pool ~1.8 times the readily releasable pool. Retrieval of this pool required large calcium influx, and was inhibited by blockers of calcium/calmodulin-activated calcineurin and dynamin, suggesting the involvement of calcineurin and dynamin in endocytosis overshoot. Depletion of the overshoot pool slowed down compensatory endocytosis, whereas recovery of the overshoot pool via exocytosis that deposited stranded vesicles to the plasma membrane led to recovery of compensatory endocytosis, suggesting that the overshoot pool enhances endocytosis efficiency. These results suggest that the overshoot pool exists at every nerve terminal, is of limited size arising from vesicles stranded at the plasma membrane, is retrieved via calcium/calmodulin/calcineurin and dynamin signaling pathway, and can enhance endocytosis efficiency. Potential mechanisms for how the endocytosis overshoot pool enhances endocytosis efficiency are discussed.

Introduction

Endocytosis overshoot, which retrieves more membrane than vesicles just being exocytosed, has been observed in non-neuronal secretory cells and nerve terminals (Thomas et al., 1994; Smith and Neher, 1997; Renden and von Gersdorff, 2007; Wu et al., 2009). However, it is only observed in a fraction of cells, raising a question as to its popularity. Likely because of this reason, the mechanism mediating retrieval of the overshoot membrane pool and the role of this pool are poorly understood. Early works consider calcium as a potential trigger of endocytosis overshoot (Thomas et al., 1994; Smith and Neher, 1997). Recent observation that the overshoot takes place most often after larger calcium influx and is blocked by the calcium buffer EGTA suggests that calcium influx triggers endocytosis overshoot (Wu et al., 2009). A calmodulin blocker inhibits the endocytosis overshoot, suggesting that calmodulin is involved in endocytosis overshoot (Wu et al., 2009). In addition to calcium/calmodulin, little is known about the mechanisms mediating endocytosis overshoot. For example, it remains unclear whether calcineurin, a calcium/calmodulin-activated phosphatase that dephosphorylates many endocytic proteins (Cousin and Robinson, 2001), is

involved in endocytosis overshoot. It is not known whether dynamin, the fission protein in compensatory endocytosis, is involved in endocytosis overshoot.

What generates the overshoot membrane pool? Block of dynamin-dependent endocytosis led to accumulation of a large amount of fused vesicles at the plasma membrane, which were all retrieved via dynamin-independent endocytosis overshoot, suggesting that overshoot membrane pool originates from vesicles stranded at the plasma membrane (see Wu et al., 2009, their Fig. 8). However, this observation was obtained when GTP hydrolysis was blocked. Whether it applies to control conditions remains unclear.

Endocytosis overshoot could be induced by physiological high-frequency action potential-like stimulation, suggesting that the overshoot pool is to increase the endocytosis capacity and thus to sustain synaptic transmission during high-frequency firing (Renden and von Gersdorff, 2007; Wu et al., 2009). Whether this is the only function of the overshoot pool is unclear.

We addressed the above unclear issues at the calyx nerve terminal, where overshoot can be monitored with capacitance measurements. We determined whether (1) every nerve terminal contains an overshoot membrane pool, (2) calcineurin and dynamin are involved in endocytosis overshoot, (3) endocytosis overshoot retrieves vesicles stranded at the plasma membrane, and (4) the overshoot pool enhances compensatory endocytosis efficiency.

Materials and Methods

Parasagittal brainstem slices (200 μm thick) containing the medial nucleus of the trapezoid body were prepared from 7- to 10-d-old Wistar rats
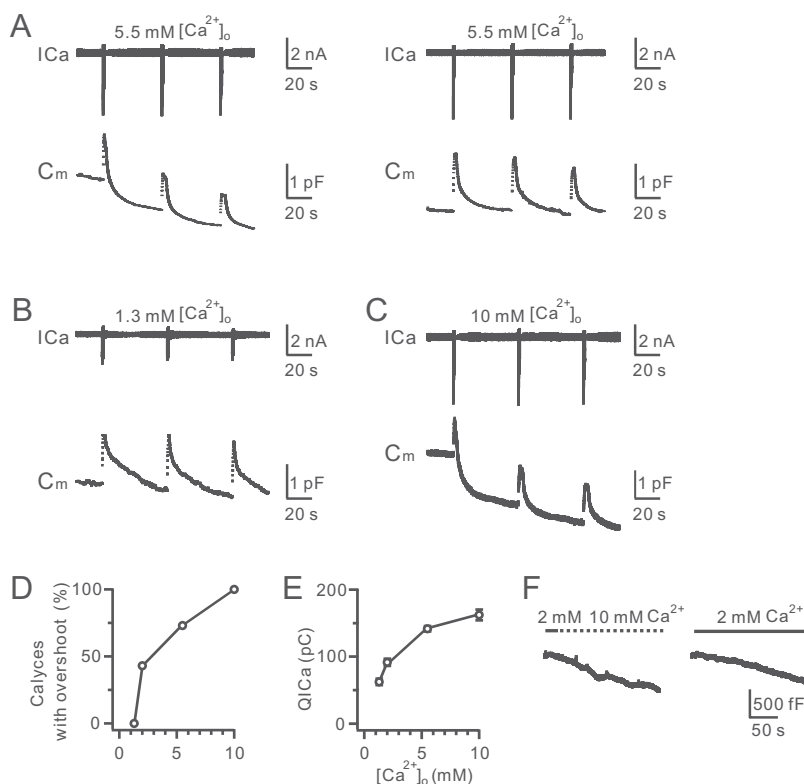
Figure 1. Overshoot pool at every calyx. **A**, Sampled I_{Ca} and membrane capacitance (C_m) induced by 3 depol$_{50 ms \times 10}$ (interval: 50 s) at $[Ca^{2+}]_o = 5.5$ mM. Overshoot was observed in the left, but not in the right panel (another calyx). **B**, **C**, Sampled I_{Ca} and C_m induced by 3 depol$_{50 ms \times 10}$ (interval: 50 s) at $[Ca^{2+}]_o = 1.3$ mM (**B**) or 10 mM (**C**). **D**, The percentage of calyces showing overshoot after 2–3 depol$_{50 ms \times 10}$ plotted versus the $[Ca^{2+}]_o$ (1.3 mM, $n = 7$; 2 mM, $n = 14$; 5.5 mM, $n = 37$; 10 mM, $n = 15$). **E**, The $Q_{I_{Ca}}$ induced by the first 50 ms depolarization during a depol$_{50 ms \times 10}$ plotted versus the $[Ca^{2+}]_o$ (1.3 mM, $n = 7$; 2 mM, $n = 14$; 5.5 mM, $n = 37$; 10 mM, $n = 15$). **F**, C_m trace at 2 mM $[Ca^{2+}]_o$ (right) or when the $[Ca^{2+}]_o$ changed from 2 to 10 mM (left).

of either sex using a vibratome. Whole-cell capacitance measurements were made with the EPC-10 amplifier together with the software lock-in amplifier (PULSE, HEKA) that implements Lindau-Neher's technique (Sun and Wu, 2001). The sinusoidal stimulus frequency was 1000 Hz, and its peak-to-peak voltage was ≤60 mV. We isolated Ca^{2+} currents with a bath solution (~22−24°C) containing (in mM): 105 NaCl, 20 TEA-Cl, 2.5 KCl, 1 MgCl$_2$, 2 or 5.5 CaCl$_2$, 25 NaHCO$_3$, 1.25 NaH$_2$PO$_4$, 25 glucose, 0.4 ascorbic acid, 3 *myo*-inositol, 2 sodium pyruvate, 0.001 tetrodotoxin, 0.1 3,4-diaminopyridine, pH 7.4, when bubbled with 95% O$_2$ and 5% CO$_2$. To increase the $[Ca^{2+}]_o$ to 10 mM, We used a HEPES solution containing (in mM): 105 NaCl, 20 TEA-Cl, 2.5 KCl, 1 MgCl$_2$, 10 CaCl$_2$, 25 dextrose, 10 HEPES, 0.4 ascorbic acid, 3 *myo*-inositol, 2 sodium pyruvate, 0.001 TTX. Application of this solution was limited to ~5−6 min and the solution was bubbled with 95% O$_2$ and 5% CO$_2$, in which we did not see any significant rundown of the electrical properties of the calyx. The presynaptic pipette contained (in mM): 125 Cs-gluconate, 20 CsCl, 4 MgATP, 10 Na$_2$-phosphocreatine, 0.3 GTP, 10 HEPES, 0.05 BAPTA, pH 7.2, adjusted with CsOH. The BAPTA concentration (50 μM) mimicked the endogenous calcium buffer capacity at calyces (Helmchen et al., 1997).

The statistical test was a *t* test. Means are presented as ±SE. The initial endocytosis rate, Rate$_{decay}$, was measured within the first 3–6 s after stimulus (Wu et al., 2009). For measuring overshoot, 2–3 depol$_{50 ms \times 10}$ (10 pulses of 50 ms depolarization to +10 mV at 10 Hz) were applied at an interval of 20–50 s. With an interval of 50 s, the overshoot amplitude was calculated as the sum of the overshoot at 40 s after each depol$_{50 ms \times 10}$. The baseline capacitance drift was corrected based on the linear fit of the baseline within 20 s before each depol$_{50 ms \times 10}$. The resulting overshoot pool size (1085 ± 110 fF, $n = 27$) in calyces showing overshoot at 5.5 mM $[Ca^{2+}]_o$ was similar to the accumulated overshoot amplitude (928 ± 83 fF, $n = 23$) measured at 20 s after 2 depol$_{50 ms \times 10}$ (interval:

20 s) at 10 mM $[Ca^{2+}]_o$, in which the small capacitance drift was neglected. Furthermore, the small drift during 2 depol$_{50 ms \times 10}$ was likely similar to the small residual overshoot that we did not measure 20 s later.

Results
Every calyx contains an endocytosis overshoot pool
To determine whether every calyx contains an endocytosis overshoot pool, we induced overshoot with 10 pulses of 50 ms depolarization (all pulses from −80 to +10 mV if not mentioned) at 10 Hz (depol$_{50 ms \times 10}$) (Wu et al., 2009) at the extracellular calcium concentration ($[Ca^{2+}]_o$) of 1.3–10 mM. At $[Ca^{2+}]_o = 5.5$ mM, repeating depol$_{50 ms \times 10}$ 2 times (interval: 20–50 s) depleted the overshoot pool (Wu et al., 2009), because the overshoot induced by the third depol$_{50 ms \times 10}$ was negligible (Fig. 1*A*). Thus, the overshoot was calculated as the sum induced by the first 2 depol$_{50 ms \times 10}$. In 27 of 37 calyces, we observed significant endocytosis overshoot (> 250 fF) of 1085 ± 110 fF ($n = 27$, Fig. 1*A*, left). In the remaining 10 calyces, overshoot was negligible (45 ± 43 fF, Fig. 1*A*, right).

As the $[Ca^{2+}]_o$ increased from 1.3 to 2, 5.5, and 10 mM, calyces showing overshoot increased from 0 (0 of 7 calyces, Fig. 1*B*) to 43% (6 of 14 calyces), 73% (27 of 37 calyces, Fig. 1*A*), and 100% (15 of 15 calyces, Fig. 1*C*; data summarized in Fig. 1*D*). The increase was accompanied by the calcium current (I_{Ca}) charge ($Q_{I_{Ca}}$) increase (Fig. 1*E*). These results suggest that every calyx contained an overshoot membrane pool, which could only be depleted by large calcium influx.

At lower $[Ca^{2+}]_o$, although we could not induce overshoot at every calyx, the overshoot pool did exist. This was because we applied 10 mM extracellular calcium after the whole-cell configuration was established (holding at −80 mV) at 2 mM $[Ca^{2+}]_o$ (Fig. 1*F*, left), which took ~1–2 min for completion. The switch to 10 mM calcium did not increase the capacitance (Fig. 1*F*, left). Instead, we observed a baseline capacitance decay ($n = 5$, Fig. 1*F*, left) similar to that at 2 mM $[Ca^{2+}]_o$ ($n = 4$, Fig. 1*F*, right). The reason for this baseline decay was unclear. Nevertheless, increasing the $[Ca^{2+}]_o$ did not deposit stranded vesicles at the plasma membrane for generating the overshoot pool. The endocytosis overshoot pool must exist before the $[Ca^{2+}]_o$ was increased to 10 mM.

Blockers of calcineurin and dynamin inhibit endocytosis overshoot
To study the role of calcineurin, we included in the pipette either the calcineurin autoinhibitory peptide (CaN$_{457−482}$, 150 μM) or cyclosporine A (CsA, 20–50 μM) (Oliveria et al., 2007). These two blockers are specific at calyces because they inhibit rapid and slow compensatory endocytosis as knocking out calcineurin A$_\alpha$ subunit at calyces (Sun et al., 2010). We induced endocytosis overshoot by 3 depol$_{50 ms \times 10}$ applied every 50 s at $[Ca^{2+}]_o = 5.5$ mM. In the presence of CaN$_{457−482}$, endocytosis overshoot was blocked
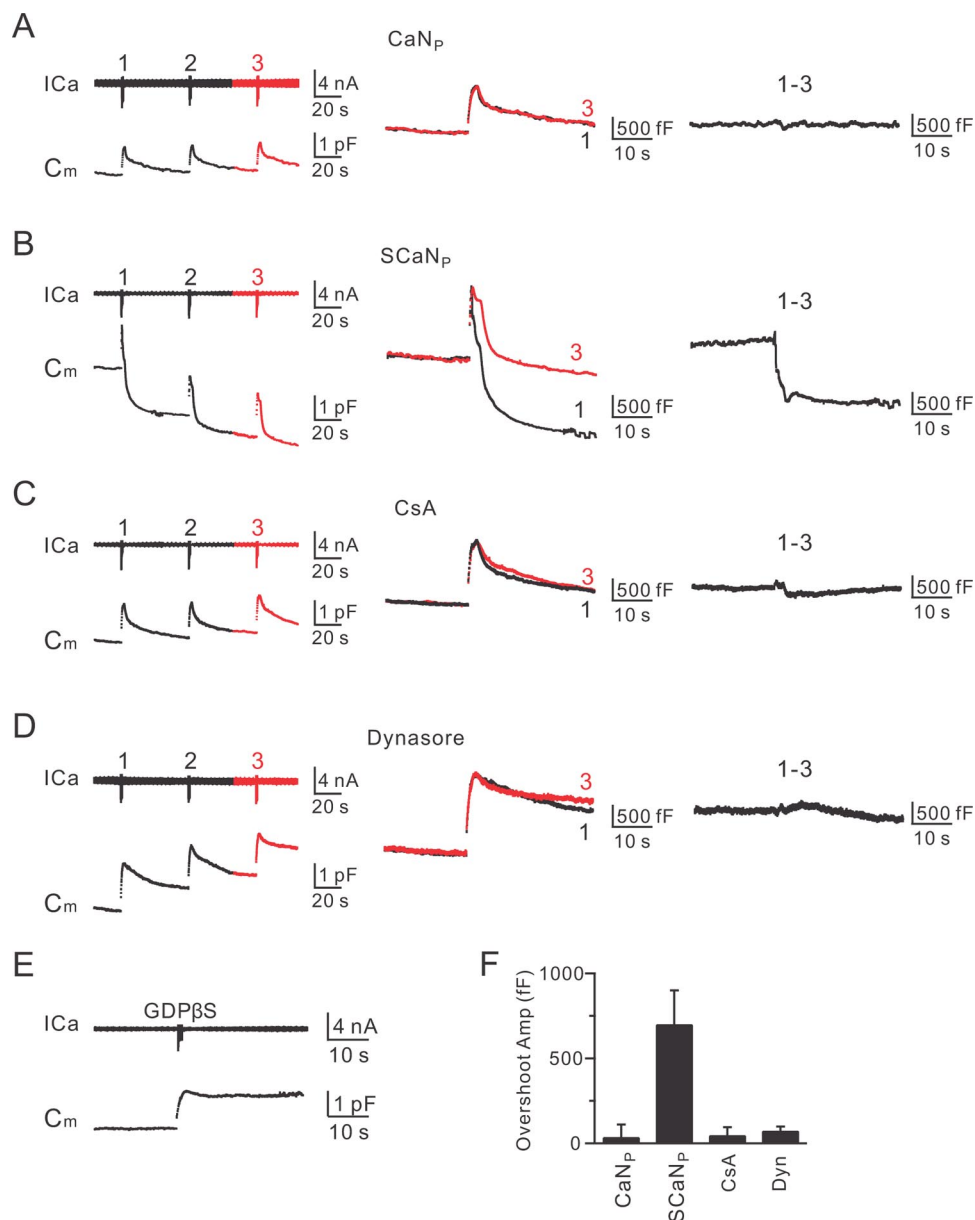
Figure 2. Calcineurin and dynamin blockers inhibit endocytosis overshoot. **A–D**, Sampled I_{Ca} and C_m induced by 3 depol$_{50\,ms}\times_{10}$ applied every 50 s in the presence of CaN$_{457-482}$ (CaN$_p$, 150 μM in pipette, **A**), scrambled CaN$_{457-482}$ (SCaN$_p$, 150 μM, **B**), CsA (20 μM in pipette, **C**), or dynasore (100 μM in pipette, **D**). C_m change induced by the third and the first depol$_{50\,ms}\times_{10}$ was superimposed (middle). Subtraction of the third C_m response from the first one yields a trace reflecting endocytosis overshoot only (right). **E**, Sampled I_{Ca} and C_m induced by a depol$_{50\,ms}\times_{10}$ in the presence of GDPβS (0.3 mM in pipette). **F**, The overshoot amplitude induced by the first depol$_{50\,ms}\times_{10}$, calculated as the difference between the first and the third C_m response (**A–D**), plotted in the presence of CaN$_p$ ($n=7$), SCaN$_p$ ($n=7$), CsA ($n=9$) or dynasore (Dyn, $n=15$).

in 7 of 7 calyces. In contrast, in the presence of scrambled CaN$_{457-482}$ (150 μM), endocytosis overshoot was observed in 6 of 7 calyces with an amplitude (1050 ± 302 fF, $n=7$, Fig. 2 B, χ^2 test, $p<$ 0.01) similar to that of the control (Fig. 1). Like CaN$_{457-482}$, CsA (20–50 μM) abolished endocytosis overshoot in 9 of 9 calyces (Fig. 2C, χ^2 test, $p<0.01$).

In the presence of CaN$_{457-482}$ or CsA, the capacitance decay was slowed down, but not abolished (Fig. 2A,C). One may argue that the capacitance decay reflected endocytosis overshoot, whereas the compensatory endocytosis was abolished. This scenario predicts that endocytosis overshoot in the presence of calcineurin blockers should be similar to control, that is, endocytosis overshoot should be induced by the first 2 depol$_{50\,ms}\times_{10}$, but not the third one. In other words, the capacitance decay induced by the first depol$_{50\,ms}\times_{10}$ should be much larger than

that by the third depol$_{50\,ms}\times_{10}$. This prediction was incorrect, as quantified below (Fig. 2A,C).

In control (with scrambled CaN$_{457-482}$), the first depol$_{50\,ms}\times_{10}$ generated an overshoot of 785 ± 236 fF ($n=7$, included calyces with or without overshoot), whereas the third depol$_{50\,ms}\times_{10}$ induced only compensatory endocytosis (Fig. 2B; see also Fig. 1A). By subtracting the capacitance decay induced by the third depol$_{50\,ms}\times_{10}$ from that by the first depol$_{50\,ms}\times_{10}$, the difference reflected purely the endocytosis overshoot with an amplitude (702 ± 198 fF, $n=7$, Fig. 2B) similar to that (785 ± 236 fF, $n=7$) measured directly from the first capacitance response. However, same subtraction in the presence of CaN$_{457-482}$ or CsA revealed negligible overshoot (Fig. 2F, CaN$_{457-482}$: 38 ± 73 fF, $n=7$; CsA: 48 ± 47 fF, $n=9$; summarized). Thus, CaN$_{457-482}$ and CsA abolished overshoot.
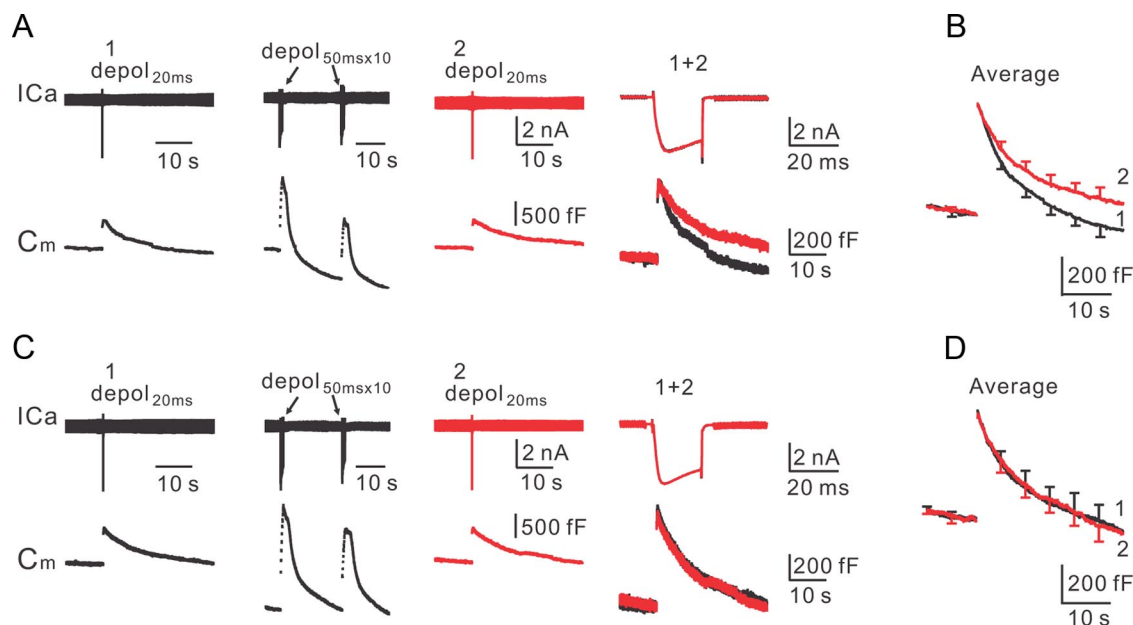
Figure 3. Overshoot pool depletion slows down endocytosis. **A**, Sampled I_{Ca} and C_m from a calyx stimulated with a depol$_{20\,ms}$ (first, black) and 40 s rest (left), 2 depol$_{50\,ms} \times 10$ (interval: 20 s, middle left), and another depol$_{20\,ms}$ 40 s later (second, middle right, red). Traces induced by first and second depol$_{20\,ms}$ are superimposed (right). **B**, The mean C_m induced by first and second depol$_{20\,ms}$ (same protocol as **A**) from 30 calyces showing significant overshoot (> 250 fF, data expressed as +SE or −SE every 5 s). **C, D**, Similar to **A** and **B**, except from 9 calyces showing no significant overshoot.

Although unlikely, we could not exclude the possibility that overshoot was only partially inhibited by CaN$_{457-482}$ and CsA so that the first and the third depol$_{50\,ms} \times 10$ induced similar, yet smaller endocytosis overshoot. However, even with this scenario, our conclusion that CaN$_{457-482}$ and CsA inhibited overshoot holds.

To determine whether the GTPase dynamin is involved in endocytosis overshoot, we included in the pipette either dynasore (100 μM, Fig. 2D) or GDPβS (0.3 mM, Fig. 2E) to inhibit the GTPase activity of dynamin (Macia et al., 2006). Dynasore is specific to dynamin at calyces, because it inhibits endocytosis as dynamin I knock-out at calyces (Lou et al., 2008; Xu et al., 2008). In the presence of dynasore, 3 depol$_{50\,ms} \times 10$ applied at 50 s interval slowed down the capacitance decay and induced no overshoot ($n = 15$). Subtraction of the third response from the first response revealed that the first depol$_{50\,ms} \times 10$ induce negligible overshoot (Fig. 2D,F). GDPβS blocked overshoot, because the capacitance decay after a depol$_{50\,ms} \times 10$ was nearly abolished ($n = 5$, Fig. 2E). These results suggest the involvement of dynamin in endocytosis overshoot.

Depletion of the endocytosis overshoot pool slows down endocytosis

To determine whether the overshoot pool enhances endocytosis efficiency, we applied a stimulation protocol composed of a 20 ms depolarization (depol$_{20\,ms}$) and 40 s rest for measuring the endocytosis rate, 2 depol$_{50\,ms} \times 10$ (interval: 20 s) to deplete the overshoot pool, and another depol$_{20\,ms}$ (second) applied at 40 s after the second depol$_{50\,ms} \times 10$ for measuring the endocytosis rate (Fig. 3A). The $[Ca^{2+}]_o$ was 5.5 mM. The first depol$_{20\,ms}$, which depletes the readily releasable vesicle pool (Sun and Wu, 2001), induced a capacitance jump (ΔC_m) of 541 $\pm$ 20 fF ($n = 39$, e.g., Fig. 3A, left). The jump was followed by a monoexponential decay with a τ of 10.9 $\pm$ 0.7 s in 35 calyces, and by a biexponential decay in 4 calyces with τ of 0.4 $\pm$ 0.2 s (25 $\pm$ 4%) and 8.9 $\pm$ 1.6 s, respectively. The initial capacitance decay, which reflects the initial endocytosis rate (Rate$_{endo}$, measured within 3–6 s after stimula-

tion), was 76 $\pm$ 8 fF/s ($n = 39$, Fig. 3A, left). Subsequent 2 depol$_{50\,ms} \times 10$ depleted the overshoot pool in 30 of 39 calyces with an overshoot amplitude of 1018 $\pm$ 104 fF ($n = 30$, Fig. 3A). The second depol$_{20\,ms}$, induced a ΔC_m (528 $\pm$ 24 fF, $n = 30$) similar to that by the first depol$_{20\,ms}$, but a Rate$_{endo}$ (53 $\pm$ 5 fF/s, $n = 30$, $p < 0.01$) significantly slower than that by the first depol$_{20\,ms}$ (Fig. 3A, see B for the average). The τ was difficult to quantify because of the slow endocytosis time course, which sometimes did not return to the baseline (Fig. 3A,B). The $Q_{I_{Ca}}$ induced by the first (66.2 $\pm$ 2.4 pC, $n = 30$) and the second depol$_{20\,ms}$ (63.6 $\pm$ 2.3 pC, $n = 30$) were similar ($p > 0.9$, Fig. 3A).

In 9 of 39 calyces, repeated depol$_{50\,ms} \times 10$ induced negligible overshoot (28 $\pm$ 16 fF, $n = 9$, Fig. 3C,D). The $Q_{I_{Ca}}$, ΔC_m, endocytosis τ, and Rate$_{endo}$ induced by the first depol$_{20\,ms}$ (64.7 $\pm$ 5.7 pC, 512 $\pm$ 36 fF, 11.4 $\pm$ 0.9 s, 69 $\pm$ 10 fF/s, $n = 9$) were similar to those induced by the second depol$_{20\,ms}$ (62.9 $\pm$ 5.4 pC, 501 $\pm$ 28 fF, 11.9 $\pm$ 1.2 s, 67 $\pm$ 9 fF/s, $n = 9$; $p > 0.5$, Fig. 3C,D). These results suggest that overshoot pool depletion slows down the Rate$_{endo}$.

Recovery of the overshoot pool and endocytosis efficiency

To determine whether the overshoot pool and the Rate$_{endo}$ could recover, we applied a stimulation protocol composed of (1) first depol$_{20\,ms}$ and a 35 s rest, (2) 2 depol$_{50\,ms} \times 10$ (interval: 20 s) and a 45 s rest, (3) either 90 s rest (Fig. 4A, control protocol) or 6 pulses of 20 ms depolarization from −80 to −5 mV at 10 s interpulse interval and a 40 s rest (Fig. 4B, test protocol), (4) second depol$_{20\,ms}$ and 35 s rest, and (5) 2 depol$_{50\,ms} \times 10$ (interval: 20 s). The $[Ca^{2+}]_o$ was 10 mM. The overshoot induced by the first 2 depol$_{50\,ms} \times 10$ was 928 $\pm$ 83 fF ($n = 23$), which was 1.8 $\pm$ 0.2 ($n = 23$) times the readily releasable pool size, the ΔC_m induced by a depol$_{20\,ms}$ (Fig. 4A).

For the control protocol (Fig. 4A, without 6 depolarizing pulses), Rate$_{endo}$ (43 $\pm$ 4 fF/s, $n = 7$) induced by the second depol$_{20\,ms}$ was significantly smaller than the first one (62 $\pm$ 5 fF/s, $n = 7$, $p < 0.01$, Fig. 4A), consistent with results shown in Figure 3. The overshoot induced by the second train of 2 depol$_{50\,ms} \times 10$
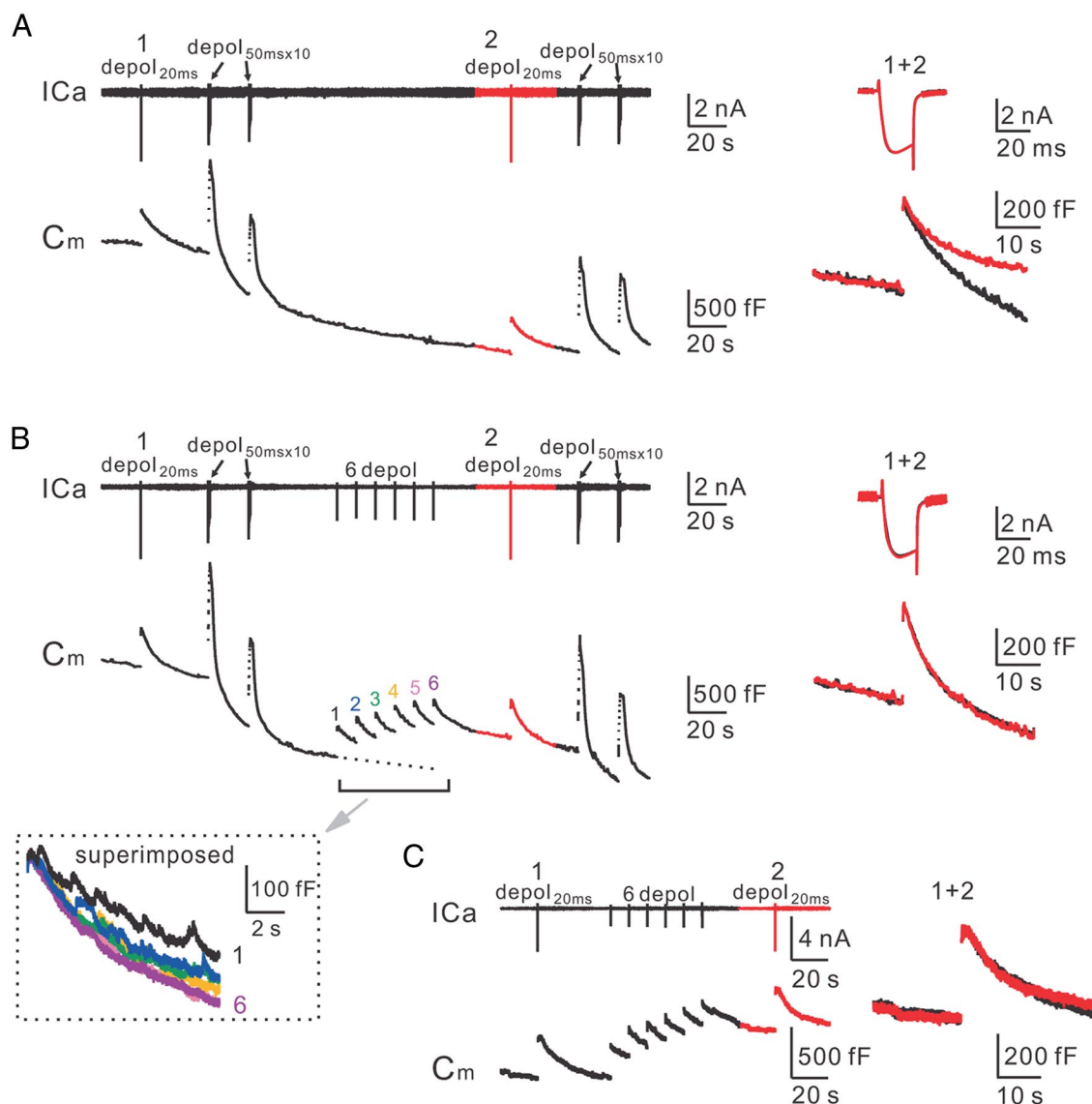
Figure 4. Recovery of the overshoot pool and endocytosis rate. ***A***, ***B***, Left, Mean I_{Ca} and C_m stimulated with a control (***A***, $n = 7$) or test (***B***, $n = 16$) protocol described in Results. The dotted line (***B***) is an extrapolation of the capacitance drift. The inset in ***B*** shows the capacitance decay after 6 depolarizing pulses (traces are colored-coded and superimposed). The decay is faster as the pulse number increases. Right, I_{Ca} and C_m induced by first (black) and second (red) $depol_{20\ ms}$ are superimposed. ***C***, Sampled I_{Ca} and C_m induced by a $depol_{20\ ms}$ (first), 6 depolarizing pulses (interval: 10 s) and another $depol_{20\ ms}$ (second). Responses to first and second $depol_{20\ ms}$ are also superimposed (right).

was only $8 \pm 5\%$ ($n = 7$) of that induced by the first train (Fig. 4*A*), indicating negligible overshoot recovery.

For the test protocol (Fig. 4*B*, with 6 depolarizing pulses), the $Rate_{endo}$ induced by the second $depol_{20\ ms}$ (75 ± 6 fF/s, $n = 16$) was similar to that induced by the first $depol_{20\ ms}$ (78 ± 7 fF/s, $n = 16$, $p > 0.9$), and the overshoot induced by the second train of 2 $depol_{50\ ms \times 10}$ was $50 \pm 6\%$ ($n = 16$) of that induced by the first train (Fig. 4*B*). The ΔC_m, the endocytosis time constant(s) and $Q_{I_{Ca}}$ induced by the second $depol_{20\ ms}$ were similar to those induced by the first $depol_{20\ ms}$ ($n = 16$, $p > 0.9$; Fig. 4*B*). Thus, after overshoot pool depletion, vesicle fusion during 6 depolarizing pulses (Fig. 4*B*) led to partial overshoot pool recovery and the $Rate_{endo}$ recovery, suggesting that overshoot pool recovery causes the $Rate_{endo}$ recovery.

Partial overshoot recovery predicted that 6 depolarizing pulses generated stranded vesicles at the plasma membrane. As measured 125 s after the onset of 6 depolarizing pulses, the capacitance increased by 71 ± 41 fF ($n = 16$, Fig. 4*B*, dotted line). In

contrast, the capacitance decreased by 443 ± 54 fF ($n = 7$) at the same time frame, but without 6 depolarizing pulses (Fig. 4*A*, dotted line). Thus, 6 depolarizing pulses generated ~514 fF of stranded vesicles at the plasma membrane, similar to the recovered overshoot amplitude (460 ± 23 fF, $n = 16$). The capacitance decrease in the absence of depolarization (Fig. 4*A*) was due to baseline drift, because a similar drift (568 ± 101 fF, $n = 5$) was observed during the same time frame (125 s) of whole-cell recordings at 10 mM $[Ca^{2+}]_o$ (Fig. 1*F*, left). In addition, residual endocytosis overshoot, which was not completed at 20 s after 2 $depol_{50\ ms \times 10}$, might contribute to the drift to a minor extent.

During 6 depolarizing pulses, endocytosis rate after each pulse increased gradually (Fig. 4*B*, inset). This is consistent with the increase of stranded vesicles that may enhance endocytosis, although it might be also due to accumulation of fused vesicles that recruit more endocytic sites for retrieval (Balaji et al., 2008).

While recovery of the overshoot and $Rate_{decay}$ after 6 depolarizing pulses (Fig. 4) suggests a casual relation between the over-

shoot pool and Rate$_{decay}$, an alternative explanation is that residual calcium generated by 6 depolarizing pulses facilitates Rate$_{decay}$. This explanation is unlikely for three reasons. First, residual calcium generated by each 20 ms depolarization lasted for only ~1 s ($n = 5$, our unpublished data; see also Wu and Borst, 1999). There should be no residual calcium at 40 s after 6 depolarizing pulses, at which time we measured Rate$_{decay}$. Second, despite using stimuli (e.g., 10 pulses of 20 ms depolarization at 10 Hz) much stronger than 6 depolarizing pulses, the Rate$_{decay}$ measured 40 s later did not increase (Xu et al., 2008; Wu et al., 2009), suggesting that residual calcium 40 s later does not facilitate endocytosis. Third, without preceding depol$_{50\ ms\ \times\ 10}$, the Rate$_{decay}$ induced by a depol$_{20\ ms}$ 40 s before and after the 6 depolarizing pulses did not change significantly (Fig. 4C, $n = 5$, $p > 0.8$), indicating that 6 depolarizing pulses alone could not increase Rate$_{decay}$.

Could the overshoot pool recovery (Fig. 4B) be due to residual calcium rather than stranded vesicles produced by 6 depolarizing pulses? This possibility is unlikely for three reasons. First, when GDPβS blocks dynamin-dependent endocytosis (Xu et al., 2008), stimulation (11 depol$_{20\ ms}$ at 0.1 Hz) induced 3.2 ± 0.6 pF ($n = 5$) of stranded vesicle membrane at the plasma membrane (Wu et al., 2009). Subsequent strong stimulation induced dynamin-independent endocytosis and an endocytosis overshoot (2.5 ± 0.6 pF, $n = 5$) similar to the accumulated stranded vesicles, indicating that the overshoot is from stranded vesicles (Wu et al., 2009). Consistently, stranded vesicles produced by 6 depolarizing pulses (~514 fF) were similar to the recovered overshoot size (460 ± 23 fF, $n = 16$, Fig. 4B). Second, regardless of the preceding stimuli, as long as they induced compensatory endocytosis, subsequent 2–3 depol$_{50\ ms\ \times\ 10}$ did not induce a larger overshoot than those without the preceding stimuli, suggesting that residual calcium alone could not increase overshoot. Third, when the interval of 6 depolarizing pulses was increased to 20 s, the overshoot pool recovery was similar to that with an interval of 10 s ($n = 6$, data not shown).

Discussion

Our results can be summarized in four aspects. First, previous reports of endocytosis overshoot from only a fraction of cells question whether overshoot is a widespread phenomenon. We found that every nerve terminal contained an overshoot pool ~1.8 times the readily releasable pool, retrieval of which required large calcium influx (Fig. 1). As calcium influx increased, the fraction of calyces showing overshoot increased (Fig. 1), explaining why overshoot is usually reported from a fraction of cells. Thus, endocytosis overshoot is a widespread phenomenon at nerve terminals. As the $[Ca^{2+}]_o$ approached the physiological level of 1.3–2 mM, overshoot was more difficult to induce (Fig. 1), suggesting that the overshoot pool is preserved in many physiological conditions, which may ensure its role in enhancing the endocytosis efficiency.

Second, although endocytosis overshoot retrieves vesicles stranded at the plasma membrane when dynamin-dependent endocytosis is blocked (Wu et al., 2009), it was unclear whether this finding applies to control conditions. The present work showed that in control, fused, but stranded vesicles replenished the overshoot pool after the pool was depleted (Fig. 4). Together, these results suggest stranded vesicles as the source for endocytosis overshoot. Stranded vesicles may be generated in resting or low calcium conditions, in which exocytosis is followed by extremely slow or no endocytosis (von Gersdorff and Matthews, 1994; Hosoi et al., 2009; Wu et al., 2009).

Third, except that calcium/calmodulin was recently found to be involved in endocytosis overshoot (Wu et al., 2009), the mechanism mediating endocytosis overshoot was unclear. We found that calcineurin and dynamin blockers inhibited overshoot. The blockers were specific, because their effects on compensatory endocytosis were confirmed with knock-out of calcineurin and dynamin (Lou et al., 2008; Xu et al., 2008; Sun et al., 2010). Thus, we found two critical molecules, calcineurin and dynamin, in mediating endocytosis overshoot. We suggest that calcium binding with calmodulin activates calcineurin, which dephosphorylates endocytosis proteins, including dynamin (Cousin and Robinson, 2001), leading to the trigger of endocytosis overshoot. Since calcium/calmodulin/calcineurin and dynamin are also involved in rapid and slow compensatory endocytosis at p7–10 calyces examined here (Yamashita et al., 2005, 2010; Xu et al., 2008; Sun et al., 2010), endocytosis overshoot and compensatory endocytosis are mediated by similar mechanisms, except that endocytosis overshoot requires larger calcium influx.

The slow calcium buffer EGTA blocks endocytosis overshoot, but only slows down compensatory endocytosis, whereas the fast calcium buffer BAPTA blocks both overshoot and compensatory endocytosis (Wu et al., 2009). These findings, together with the observed increase of the overshoot frequency at higher calcium influx (Fig. 1), suggest that endocytosis overshoot may be mediated at a place with a mean distance farther from calcium channels. However, a fraction of the overshoot pool membrane might be still near calcium channels to compete with newly exocytosed vesicles for retrieval (more discussion later).

We have previously shown that rapid and slow endocytosis are dynamin dependent, but become dynamin independent after block of dynamin with GDPβS or GTPγS when a large number of fused vesicles are accumulated at the plasma membrane (Xu et al., 2008). Similarly, endocytosis overshoot is dynamin dependent as shown here (Fig. 2), but becomes GTP independent and thus dynamin independent after block of dynamin with GDPβS when many fused vesicles are accumulated at the plasma membrane (Wu et al., 2009). Thus, similar to rapid and slow endocytosis (Xu et al., 2008), endocytosis overshoot could also be dynamin dependent and independent. Different vesicle pools that use dynamin or an unidentified fission molecule for fission might provide an explanation for the existence of dynamin-dependent and -independent forms of rapid, slow and overshoot endocytosis.

Fourth, overshoot pool depletion slowed down slow endocytosis (Figs. 3,4), the dominant form of clathrin-dependent endocytosis at synapses (Granseth et al., 2006; Kim and Ryan, 2009). After overshoot pool depletion, recovery of the overshoot pool by depositing stranded vesicles at the plasma membrane led to recovery of Rate$_{decay}$ (Fig. 4), suggesting that the overshoot pool enhances endocytosis efficiency.

We proposed that stranded vesicles at the plasma membrane compete with newly exocytosed vesicles for retrieval. It is possible that stranded vesicle membrane forms a preassembled vesicular structure, which may be advantageous for retrieval by saving many steps involved in retrieving newly exocytosed vesicles, such as sorting and transportation of membrane and proteins to endocytic sites, and membrane invagination. While it seems more likely for stranded vesicles to be retrieved, newly exocytosed vesicles can also be retrieved. Consistent with this possibility, endocytosis induced by depol$_{20\ ms}$ was slower but not abolished after overshoot pool depletion (Figs. 3,4). Endocytosis induced by a depol$_{50\ ms\ \times\ 10}$ also slowed down after overshoot pool depletion, but was still much faster than that induced by depol$_{20\ ms}$ (Figs.

3,4), in agreement with regulation of endocytosis by calcium (Sankaranarayanan and Ryan, 2001; Hosoi et al., 2009; Wu et al., 2009).

In summary, using capacitance measurements to monitor vesicle's lipid membrane turnover, the present work suggests that the overshoot pool exists at every nerve terminal, is of limited size arising from vesicles stranded at the plasma membrane, is retrieved via calcium/calmodulin/calcineurin and dynamin signaling pathway, and can enhance endocytosis efficiency. These findings complement recent observation of a plasma membrane pool of vesicle proteins, including synaptotagmin, VAMP2, synaptophysin, and the vesicular glutamate transporter vGlu1, which may be preferentially retrieved (but see Willig et al., 2006; Fernández-Alfonso et al., 2006; Wienisch and Klingauf, 2006; Hua et al., 2011).

Endocytosis overshoot could be induced by physiological high-frequency action potential-like stimulation, suggesting that the overshoot pool increases the endocytosis capacity during high-frequency firing (Renden and von Gersdorff, 2007; Wu et al., 2009). The present work suggests that the overshoot pool can also enhance the efficiency of compensatory endocytosis. These functions may help nerve terminals with a limited number of recycling vesicles to maintain synaptic transmission during repetitive firing. Although these functions were found in calyces, their significance is likely to apply beyond calyces, because endocytosis overshoot was found at other nerve terminals and endocrine cells (Thomas et al., 1994; Hsu and Jackson, 1996; Smith and Neher, 1997).

References

Balaji J, Armbruster M, Ryan TA (2008) Calcium control of endocytic capacity at a CNS synapse. J Neurosci 28:6742–6749.

Cousin MA, Robinson PJ (2001) The dephosphins: dephosphorylation by calcineurin triggers synaptic vesicle endocytosis. Trends Neurosci 24:659–665.

Fernández-Alfonso T, Kwan R, Ryan TA (2006) Synaptic vesicles interchange their membrane proteins with a large surface reservoir during recycling. Neuron 51:179–186.

Granseth B, Odermatt B, Royle SJ, Lagnado L (2006) Clathrin-mediated endocytosis is the dominant mechanism of vesicle retrieval at hippocampal synapses. Neuron 51:773–786.

Helmchen F, Borst JG, Sakmann B (1997) Calcium dynamics associated with a single action potential in a CNS presynaptic terminal. Biophys J 72:1458–1471.

Hosoi N, Holt M, Sakaba T (2009) Calcium dependence of exo- and endocytotic coupling at a glutamatergic synapse. Neuron 63:216–229.

Hsu SF, Jackson MB (1996) Rapid exocytosis and endocytosis in nerve terminals of the rat posterior pituitary. J Physiol 492:539–553.

Hua Y, Sinha R, Thiel CS, Schmidt R, Hüve J, Martens H, Hell SW, Egner A, Klingauf J (2011) A readily retrievable pool of synaptic vesicles. Nat Neurosci 14:833–839.

Kim SH, Ryan TA (2009) Synaptic vesicle recycling at CNS synapses without AP-2. J Neurosci 29:3865–3874.

Lou X, Paradise S, Ferguson SM, De Camilli P (2008) Selective saturation of slow endocytosis at a giant glutamatergic central synapse lacking dynamin 1. Proc Natl Acad Sci U S A 105:17555–17560.

Macia E, Ehrlich M, Massol R, Boucrot E, Brunner C, Kirchhausen T (2006) Dynasore, a cell-permeable inhibitor of dynamin. Dev Cell 10:839–850.

Oliveria SF, Dell'Acqua ML, Sather WA (2007) AKAP79/150 anchoring of calcineurin controls neuronal L-type Ca^{2+} channel activity and nuclear signaling. Neuron 55:261–275.

Renden R, von Gersdorff H (2007) Synaptic vesicle endocytosis at a CNS nerve terminal: faster kinetics at physiological temperatures and increased endocytotic capacity during maturation. J Neurophysiol 98:3349–3359.

Sankaranarayanan S, Ryan TA (2001) Calcium accelerates endocytosis of vSNAREs at hippocampal synapses. Nat Neurosci 4:129–136.

Smith C, Neher E (1997) Multiple forms of endocytosis in bovine adrenal chromaffin cells. J Cell Biol 139:885–894.

Sun JY, Wu LG (2001) Fast kinetics of exocytosis revealed by simultaneous measurements of presynaptic capacitance and postsynatpic currents at a central synapse. Neuron 30:171–182.

Sun T, Wu XS, Xu J, McNeil BD, Pang ZP, Yang W, Bai L, Qadri S, Molkentin JD, Yue DT, Wu LG (2010) The role of calcium/calmodulin-activated calcineurin in rapid and slow endocytosis at central synapses. J Neurosci 30:11838–11847.

Thomas P, Lee AK, Wong JG, Almers W (1994) A triggered mechanism retrieves membrane in seconds after Ca^{2+}-stimulated exocytosis in single pituitary cells. J Cell Biol 124:667–675.

von Gersdorff H, Matthews G (1994) Inhibition of endocytosis by elevated internal calcium in a synaptic terminal. Nature 370:652–655.

Wienisch M, Klingauf J (2006) Vesicular proteins exocytosed and subsequently retrieved by compensatory endocytosis are nonidentical. Nat Neurosci 9:1019–1027.

Willig KI, Rizzoli SO, Westphal V, Jahn R, Hell SW (2006) STED microscopy reveals that synaptotagmin remains clustered after synaptic vesicle exocytosis. Nature 440:935–939.

Wu LG, Borst JG (1999) The reduced release probability of releasable vesicles during recovery from short-term synaptic depression. Neuron 23:821–832.

Wu XS, McNeil BD, Xu J, Fan J, Xue L, Melicoff E, Adachi R, Bai L, Wu LG (2009) Ca(2+) and calmodulin initiate all forms of endocytosis during depolarization at a nerve terminal. Nat Neurosci 12:1003–1010.

Xu J, McNeil B, Wu W, Nees D, Bai L, Wu LG (2008) GTP-independent rapid and slow endocytosis at a central synapse. Nat Neurosci 11:45–53.

Yamashita T, Hige T, Takahashi T (2005) Vesicle endocytosis requires dynamin-dependent GTP hydrolysis at a fast CNS synapse. Science 307:124–127.

Yamashita T, Eguchi K, Saitoh N, von Gersdorff H, Takahashi T (2010) Developmental shift to a mechanism of synaptic vesicle endocytosis requiring nanodomain Ca^{2+}. Nat Neurosci 13:838–844.